# Polarimetric Radar Measurements of Tropical Rain at a 5-cm Wavelength

P. T. MAY AND T. D. KEENAN

*Bureau of Meterology Research Centre, Melbourne, Victoria, Australia*

D. S. ZRNIĆ

*NOAA/Environmental Research Laboratories, National Severe Storms Laboratory, Norman, Oklahoma*

L. D. CAREY AND S. A. RUTLEDGE

*Department of Atmospheric Science, Colorado State University, Fort Collins, Colorado*

(Manuscript received 1 December 1997, in final form 8 July 1998)

ABSTRACT

A 5-cm wavelength (C band) polarimetric radar was deployed during the MCTEX (Maritime Continent Thunderstorm Experiment) field program. This paper investigates the use of the C-band data for quantitative rainfall measurements with particular emphasis on specific differential phase ($K_{DP}$) and traditional reflectivity-based rain-rate estimates in moderate to high rain rates (10–200 mm $h^{-1}$). Large values of backscatter differential phase shift are occasionally seen in these data, thus resonance scattering effects are important. A consensus algorithm for $K_{DP}$ estimation in these cases is described. The rain-rate estimates are compared with the data from a d-scale rain gauge network. The $K_{DP}$ estimates are shown to produce the highest quality data, although variations in drop size distribution characteristics have a significant effect on the rain estimates. When corrections are applied for beam blockage and attenuation, good agreement can also be obtained with $Z$–$R$-based estimates. The attenuation corrections were made using a polarimetric variable, total differential phase, which provides an estimate of the total water content along the path. The polarimetric estimates of total accumulation also show excellent agreement.

## 1. Introduction

Traditional approaches to radar rainfall estimation rely upon the correlation between the radar reflectivity ($Z$) and rainfall rate ($R$). However, over the last 40 years of radar-based rainfall estimation studies a proliferation of such $Z$–$R$ relations has developed, as indicated by the summary provided in Battan (1973). Drop size distribution (DSD) variability, meteorological variations, and instrumental factors (e.g., calibration), as described by Zawadzki (1986), are generally considered to have contributed to the failure of these traditional techniques to provide robust estimates of rainfall. The fact that raindrops are not spherical led Seliga and Bringi (1976) to propose polarimetric radar techniques as an alternative approach to rainfall estimation. They suggested the use of the differential reflectivity ($Z_{DR}$) and horizontal reflectivity ($Z_H$) for estimating the two parameters of the Marshall–Palmer (1948) DSD, hence providing a rainfall rate estimate. This general approach was further explored in most early polarimetric rainfall estimation studies. For example, the sensitivities of these $Z_H$- and $Z_{DR}$-based approaches to DSD variability were investigated by Ulbrich and Atlas (1984), and gauge-type validation studies were undertaken by Seliga et al. (1981), Bringi et al. (1982), Aydin et al. (1987), and Gorgucci et al. (1996).

The fact that the difference in the two-way phase change between horizontally and vertically polarized waves ($\Phi_{DP}$) increases with distance through rain is another basis for polarimetric-based rainfall estimation (Seliga and Bringi 1978; Mueller 1984; Sachidananda and Zrnić 1987). As discussed by Zrnić and Ryzhkov (1996), use of specific differential phase shift ($K_{DP}$) has many practical advantages. It is less susceptible to variations in DSD, does not depend on absolute radar calibration, is not affected by attenuation, is immune to beam blockage effects, and can be used to detect anomalous propagation and mixed phase conditions. However, as pointed out by Chandrasekar et al. (1990) and Keenan et al. (1997), it is susceptible to the assumed form of the relation between the raindrop axial ratio and

*Corresponding author address:* Dr. P. T. May, Bureau of Meteorology Research Centre, GPO Box 1289K, Melbourne, Victoria 3001, Australia.
E-mail: p.may@bom.gov.au

the equivalent diameter. Bringi et al. (1978) and Scarchilli et al. (1993) also propose that $\Phi_{DP}$ be employed for attenuation correction in rainfall estimation studies.

As discussed by Jameson (1991a), each microwave technique has its own potential advantages and disadvantages and minimization of the rainfall estimation error would probably require simultaneous use of more than one technique. At S band (10-cm wavelength) his results suggest that for $R < 50$ mm h$^{-1}$, $Z_{DR}$ and $Z_H$ should be employed. For $R > 50$ mm h$^{-1}$, $K_{DP}$ and $Z_{DR}$ should be employed. The results of Sachidanda and Zrnić (1986) and Chandrasekar et al. (1993) offer general support for these ideas. This combination of approaches is primarily dictated by the relation of the polarimetric variables to $R$ through their inherent relation to DSD as well as the inability of the radars, due to inherent statistical errors, to undertake the required measurements.

Not suprisingly, with the advent of polarimetric radars that can obtain $K_{DP}$ estimates this latter approach to rainfall estimation has been actively pursued in recent years. Goddard and Cherry (1984), Blackman and Illingworth (1995), Ryzhkov and Zrnić (1995a), Ryzhkov and Zrnić (1996), and others have presented rainfall estimation results based on the use of $K_{DP}$ that are extremely promising.

The purpose of this paper is to further explore the use of polarimetric and conventional radar rainfall estimation techniques in a high rainfall tropical regime using the C-band (5-cm wavelength) polarimetric (C-POL) radar described by Keenan et al. (1998). To date, with the exception of European-based work (e.g., Meischner et al. 1991), most polarimetric radars have undertaken rainfall measurements at 10-cm wavelengths (S band). Compared to S-band platforms, C-band radars have some advantages. A narrow beam is achieved with a smaller dish, which in turn means less wind loading and hence less demands on the system design (i.e., overall the system is less expensive and is more easily made portable). Furthermore, the propagation differential phase $\Phi_{DP}$ is approximately inversely proportional to wavelength, so that random statistical errors of $K_{DP}$ are less for a given rain rate and hence more accurate measurements can be made at lower rain rates. However the cost is the increase in attenuation and the potential that resonance-scattering effects could distort the measurements, especially in tropical regimes where large raindrops are known to occur (Keenan et al. 1998).

Attenuation at the 5-cm wavelength is especially significant for conventional approaches although attenuation correction schemes can be invoked (e.g., Hildebrand 1978). However, such schemes are often unstable due to variability in reflectivity–attenuation relations and in practice have found limited application. The polarimetric-based techniques proposed by Holt (1988) and Bringi et al. (1978) offer an alternative means for correcting for such attenuation. They employ $\Phi_{DP}$ to correct for attenuation as a function of range although the error is an increasing function of range. The sensitivity of these techniques at C band to DSD effects was discussed by Jameson (1991b), who showed that substantial improvements can be made compared with iterative procedures. He estimated that without the $\Phi_{DP}$-based correction, at $R = 50$ mm h$^{-1}$, a 1-dB bias in $Z_H$ would occur with a penetration distance of 4 km. With the attenuation correction this value is increased to 40 km. However, these results still have a significant dependence on the assumed DSD characteristics and are valid only for Rayleigh scattering. Keenan et al. (1998) show that resonance scattering associated with large drop occurrence can increase attenuation by an order of magnitude, which is well above the values assumed by Jameson (1991b). In addition, the assumed raindrop axial ratio relation can bias the attenuation estimates. Measurements at 3-cm wavelengths (X band) incur even greater problems as the diameters of much of the significant DSD in moderate to heavy rainfall are in the resonance regime.

Polarimetric rainfall estimation techniques based solely on $K_{DP}$ are essentially independent of attenuation effects. However, estimation of $K_{DP}$ is affected by resonance-scattering effects, specifically through the introduction of the differential backscatter phase shift ($\delta$), which must be removed. The technical aspects of the derivation of the $K_{DP}$ estimate are therefore important, particularly at higher radar frequencies.

This paper compares single variable polarimetric and conventional approaches to rainfall estimation using C-POL data collected in the Tropics. Rainfall estimates obtained with traditional $Z$–$R$ relations with and without an attenuation correction are used as a baseline for comparison with $K_{DP}$-based polarimetric rainfall estimates and those obtained with a dense network of rain gauges. Dual variable estimators, for example, the use of combined $K_{DP}$ and $Z_{DR}$ are under study, but these require a significantly expanded analysis of differential attenuation that is beyond the scope of this paper.

## 2. Observational equipment

### *a. Radar measurements*

C-POL is a 1° beamwidth C-band polarimetric/Doppler radar capable of transmitting and receiving linear horizontal (H) and vertical (V) polarizations (Keenan et al. 1998). Using the algorithms of Zahrai and Zrnić (1993), the available polarimetric variables include $Z_{DR}$ and $\Phi_{DP}$, the correlation between H and V at zero lag [$\rho_{HV}(0)$], as well as the mean Doppler velocity and spectral width. The number of samples for extracting the polarimetric variables was 128 (64H, 64V interleaved) at a range spacing of 300 m with an azimuthal sampling of 1.0°. The pulse width is 1 $\mu$s and the pulse repetition frequency is 1000 Hz. C-POL does not employ a radome.

Data from four days (17 and 28 November, 6 and 8

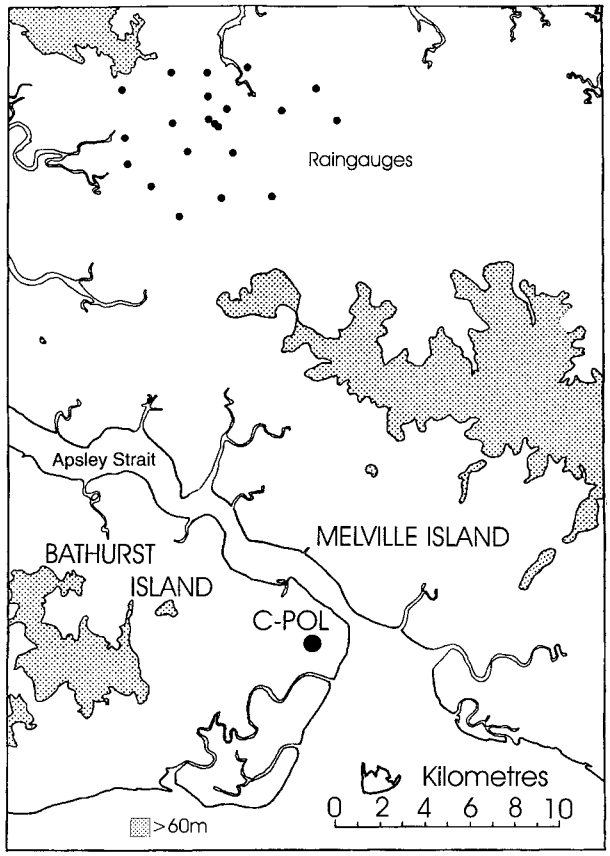


FIG. 1. The location of the C-POL radar and the dense gauge network during MCTEX. The shaded region is where the altitude exceeds 60 m.

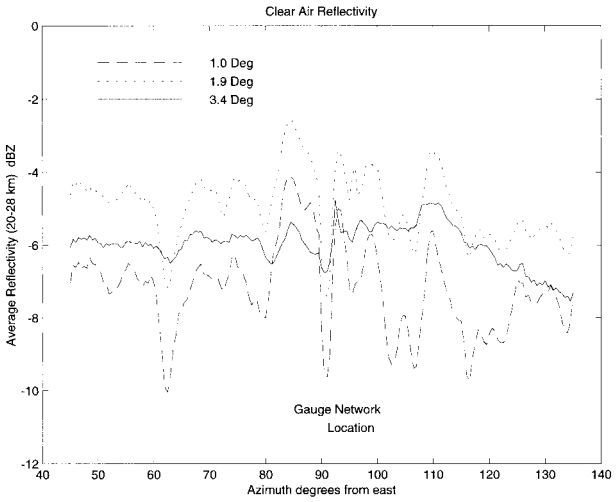


FIG. 2. Azimuthal variation of the clear-air $Z_H$ near the gauges at elevation tilts of 1.0°, 1.9°, and 3.4° averaged over 167 scans during MCTEX.

December 1995) when convective systems passed over a d-scale rain gauge network are examined herein. The data were collected during the Maritime Continent Thunderstorm Experiment (MCTEX) described by Keenan et al. (1994). The relevant MCTEX observational network is summarized in Fig. 1. C-POL was located at the Nguiu airstrip (11°45.85′S, 130°36.97′E) on the Tiwi Islands, which lie some 100 km north of Darwin, Australia. MCTEX focused on studying the characteristics and structure of the diurnally forced intense tropical thunderstorms. The observations presented here were taken from mature convective storms occurring within 30 km of the C-POL over the rain gauge network shown in Fig. 1. Storms were observed on every day of the experiment with maximum reflectivities in excess of 55 dBZ. These storms were deep (tops $>$ 16 km MSL) multicellular complexes.

For the purposes of rainfall estimation, scans from the lowest three radar elevation tilt angles are used. These are 0.7°, 2.2°, and 3.9° for 17 and 28 November; 0.7°, 1.5°, and 2.7° for 6 and 8 December 1995. In all cases radar sector scans monitoring the main area of convection were repeated every 6–8 min except for 28 November when the time interval between scans was 15 min. The most significant topographic features affecting the radar horizon included hills to the west-northwest and a 100-m elevation ridge line to the north. These features are evident in Fig. 1. The radar horizon was first deduced for the main area of interest from a topographic map. The highest obstacles at azimuths near the gauges included Tower Hill (elevation 74 m) at a range (azimuth) of 10 km (20°) giving a 0.42° horizon; a hill (elevation 80 m) at 10 km (335°) blocking to about 0.46°; a hill/escarpment (elevation 106 m) at range (azimuth) of 12 km (10°), which blocked to about 0.5°; and a ridge line (80-m elevation) extending in front of the gauges providing a horizon between 0.15° and 0.4°. However, significant close-in blockages from trees can also affect the radar measurement and appear to be dominant here.

To gain a first-order estimate of the degree to which beam blockage was affecting the radar measurements of $Z_H$, a composite of clear-air radar signatures was undertaken. It is assumed here that without blockage the average clear-air signature should be relatively uniform as a function of azimuth over the islands. There is a small decrease associated with loss in sensitivity with range. This is because we are dealing with a small azimuthal span so that variations in the orientation of insects with wind direction should be small. This is supported by the relatively small variation of reflectivity as a function of azimuth at the third elevation. The resulting composites of the clear-air $Z_H$ signature have been used in assessing the azimuthal signal variation and the implied blockage effects are summarized in Fig. 2. Clutter associated with the hills to the north, northeast, and directly west of the radar is clearly evident. The lowest two tilt angles show three significant blockages over the gauge network. At the 1.0° (1.9°) tilt the maximum signal loss is up to 5 (4) dB directly north

TABLE 1. Gauge-measured characteristics of rainfall events. Note: All rainfall figures are network averages.

| Date | Duration >5 mm h$^{-1}$ (h) | Mean rain rate (mm h$^{-1}$) | Maximum rain rate (mm h$^{-1}$) | Total (mm) |
|---|---|---|---|---|
| 17 Nov 95 | 1.02 | 28.5 | 67 | 29 |
| 28 Nov 95 | 1.25 | 29.0 | 76 | 36 |
| 6 Dec 95 | 1.12 | 17.2 | 45 | 19 |
| 8 Dec 95 | 0.90 | 20.6 | 35 | 19 |

of the radar. For the 3.4° tilt angle the maximum loss is about 2 dB. The maximum signal at the upper tilt is reduced because of the vertical gradient of the (clear air) reflectivity. Note that the elevations used for the blockage calculation are not exactly those used for the storm conditions as the tilts were modified to sample the whole storm in a timely manner.

For each elevation tilt angle, a blockage correction was obtained by deducing the deviation from the maximum observed clear-air reflectivity as a function of azimuth. This deviation was then added to each measured $Z_H$ value to obtain a blockage-corrected $Z_H$.

### *b. Gauge measurements*

The MCTEX rain gauge network consisted of twenty-one 203-mm-diameter tipping-bucket rain gauges on the semiregular 2-km grid covering an area of 680 km$^2$ located some 25 km north of C-POL (Fig. 1). Each gauge was fixed approximately 300 mm above the surface. Gauge rain-rate accuracy is typically better than 5% up to rain rates of 380 mm h$^{-1}$. At each gauge site the time of accumulation of 0.2 mm of rainfall was logged. Gauge data quality control procedures included pre- and post-MCTEX rain-rate calibrations on each gauge plus an on-site accumulation calibration (with known water quantities) at the beginning and end of the 1-month experimental period. Pairwise ''buddy'' checking of MCTEX and daily accumulations was employed to reject any faulty gauge data. A Distromet RD-69 disdrometer was also located at the center of the gauge network and its 1-min rain rates were typically within 1%–2% of a collocated gauge. One-minute rain rates were derived for each gauge by a linear interpolation procedure. These data were employed for intercomparison with the radar.

The mean characteristics of the four rain events studied in this paper are summarized in Table 1. The rainfall events are of relatively short duration (~1 h) and intense, with the network average maximum rain rates ranging from 35 to 76 mm h$^{-1}$. The two December events were significantly less intense than those of November and were more maritime in nature. The analysis focuses on periods when the average rain rate over the network exceeded 5 mm h$^{-1}$ (thus excluding some periods of trailing stratiform that persisted over the gauges after the period of interest for ~30 min), which includes over 95% of the total rain accumulation.

## 3. Estimation of $K_{DP}$

The specific differential phase $K_{DP}$ estimate and the propagation differential phase $\Phi_{DP}$ are related by

$$K_{DP} = \frac{\Delta\Phi_{DP}}{2\Delta r}, \tag{1}$$

where $\Delta\Phi_{DP}$ is the propagation differential phase change over a radial distance of $\Delta r$. The determination of $K_{DP}$ by Eq. (1) must consider that radar measurements of $\Phi_{DP}$ contain contributions from random phase errors and the backscatter differential phase shift ($\delta$). Here $K_{DP}$ is also affected by $\Delta r$ over which the difference is evaluated. The random errors of $\Phi_{DP}$ are known functions of the spectral width ($\sigma_v$), $\rho_{HV}(0)$, and the dwell time (Sachidananda and Zrnić 1986).

The larger the range interval over which a $K_{DP}$ estimate is deduced, the smaller the uncertainty in the estimate. However, as discussed by Sachidananda and Zrnić (1987), this interval cannot be made too large since the assumption of rain field homogeneity ultimately breaks down. Past studies have employed various range intervals and techniques to estimate $K_{DP}$. Regression approaches were used by Golestani et al. (1989), Balakrishnan and Zrnić (1990), and Ryzhkov and Zrnić (1995a). The latter, for example, employed the slope of a regression line through $\Phi_{DP}$ estimated from 16 successive 0.24-km-spaced range gates. The overall resolution of $K_{DP}$ was therefore about 4 km. Blackman and Illingworth (1995) used differences of adjacent mean $\Phi_{DP}$ values at 32 consecutive gates to obtain a 2-km resolution; Hubbert and Bringi (1995) employed infinite impulse response and finite impulse response filter techniques to smooth such $\Phi_{DP}$ fluctuations less than 1.5 km in scale by 15 dB. If significant $\delta$ is present, the technique of Hubbert et al. (1993a) is effective in isolating it, particularly if it does not extend over many range gates. Alternatively, as discussed by Hubbert et al. (1993b), the presence of significant $\delta$ over several successive gates can present a serious problem with simple filtering techniques. The result can be a biased $K_{DP}$ estimate due to the presence of significant $\delta$ variations.

Very large $\delta$ is possible at C band in the Tropics, as shown by the simulations presented by Keenan et al. (1997) and observations of Meischner et al. (1991). This effect is manifested as a jump, typically over one or two range gates in the monotonically (in rain) increasing $\Phi_{DP}$ curve. If the phase shift is a true spike deviating from the mean trend and much greater than the measurement standard deviation of $\Phi_{DP}$, it is usually considered a $\delta$ effect. An example with a suspected $\delta$ effect in the C-POL data collected on 28 November 1995 at 0449 UTC is shown in Fig. 3. Here a 10° jump in $\Phi_{DP}$ is evident over one gate at a range of 37.5 km. The

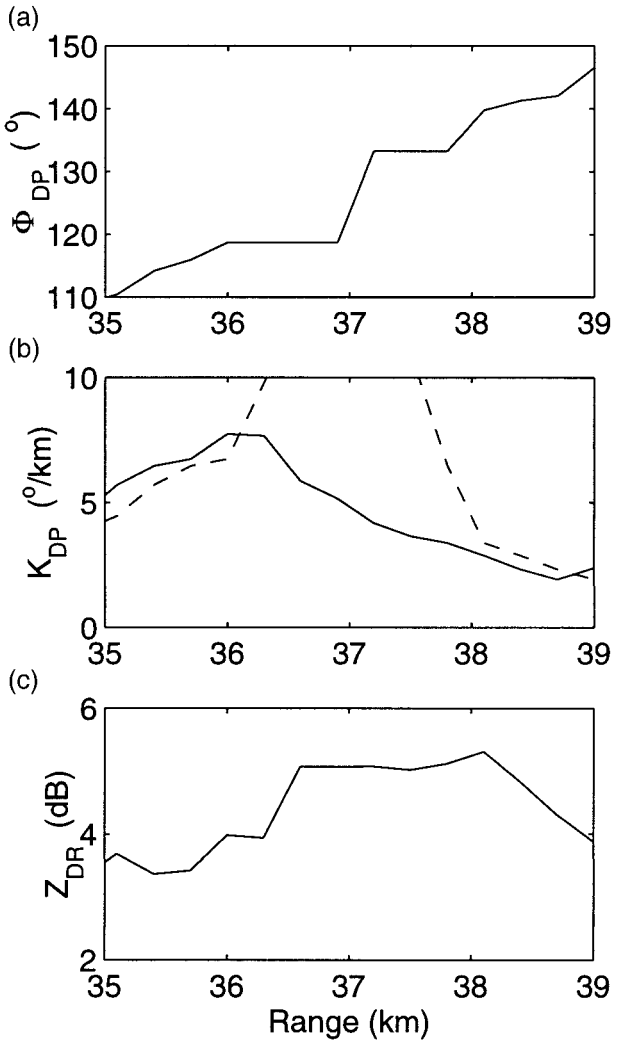


FIG. 3. (a) C-POL $\Phi_{DP}$, (b) $K_{DP}$, and (c) $Z_{DR}$ values as a function of range for a ray at an elevation of 2.2° and an azimuth of 334° at 0449 UTC 17 Nov 1995 during MCTEX. The two estimates of $K_{DP}$ correspond to a consensus estimate (solid line) and a simple least squares fit (dashed line). Large values of $K_{DP}$ occur over several gates for the least squares approach in the region of the large $\delta$, whereas consensus-based $K_{DP}$ estimates are unbiased.

effect is discernible over several azimuth angles and three scan times and occurs in a region with high $Z_{DR}$ values. Keenan et al. (1998) show that a typical value for the standard deviation of $\Phi_{DP}$ from C-POL during MCTEX is 3°–4°. The change in $\Phi_{DP}$ is therefore twice that expected from noise. In such cases a least squares fitting procedure will severely bias any $K_{DP}$ estimate, actually extending the effect introduced by $\delta$ in range.

In this paper $K_{DP}$ was estimated by first employing a nine-point median filter. This has the effect of smoothing the $\Phi_{DP}$ data but retaining persistent ($\delta$) jumps. This substantially reduced the ''noise'' in $\Phi_{DP}$ from about 3°–4° to 1°–1.5°. Then, following Fischer and Bolles (1981), a consensus estimate approach was used to overcome the problem inherent with ''outlying'' values that degrade the accuracy of least squares techniques. The consensus approach uses several estimates, each based on the minimum possible data, and then averages a subset based on the largest cluster of estimates within a predetermined interval. In this case, the $\Phi_{DP}$ slope was first estimated from each pair of adjacent values. Thus with six range gates being employed there were five estimates of the slope in $\Phi_{DP}$ available. The largest cluster that was within an interval of 5° km$^{-1}$ was then assembled and averaged. If the group contained fewer than three estimates, the data were rejected. An interval of 5° km$^{-1}$ was chosen empirically to remove large $\delta$ effects but retain smaller variations. Estimates based on noise or with $\delta$ effects were thereby eliminated from the average. In the case where all values lie within the specified interval, the least squares approach is optimal and was in fact substituted for the consensus approach.

The least squares approach and consensus estimate of $K_{DP}$ are compared for the example in Fig. 3 with significant $\delta$. Here the large $\delta$ value severely biases the $K_{DP}$ estimates by the least squares approach over several range gates. The biased estimates are large and imply rain rates in excess of 400 mm h$^{-1}$, which were not observed. In contrast the consensus average approach provides a smoothly distributed and physically realistic range variation of $K_{DP}$.

As discussed previously, the interval over which the $K_{DP}$ estimate is derived is a compromise over the desire for high spatial resolution and the need to realize a statistically stable estimate. The standard deviation of the $K_{DP}$ estimates using $N$ points is given by

$$\sigma_{K_{DP}} = \sqrt{\frac{3\sigma^2_{\Phi_{DP}}}{N(N-1)(N+1)\Delta r^2}}, \qquad (2)$$

where $\sigma^2_{\Phi_{DP}}$ is the variance of the $\Phi_{DP}$ estimates. The resulting $\sigma_{K_{DP}}$ is about 0.6° km$^{-1}$.

The relative error of the $K_{DP}$ estimates is determined partly by the rain rate; a heavy rain regime has high $K_{DP}$ values and hence a correspondingly lower relative error. As noted the range interval for the $K_{DP}$ estimation has varied typically from 1.5 to 4 km. This study is primarily concerned with high rainfall regimes, as recorded by the gauges and discussed previously. Hence three range intervals (1.2, 1.8, and 3 km) corresponding to 4, 6, and 10 range gates were employed to investigate this source of sensitivity in the $K_{DP}$ estimation. Comparison of the resultant $K_{DP}$-based rainfall estimates with the gauges indicates that the increased gate interval produced higher correlations by about 0.03 per step. This is at least partly a result of increasing the value of $N$ in Eq. (2). However, observations indicate that the MCTEX storm cells are often less than 3 km in size, and so for the remainder of this paper $K_{DP}$ will be derived over a range interval of 1.8 km (i.e., six gates).

## 4. Attenuation correction

Attenuation with C-band radar systems is significant, especially in the Tropics. With polarimetric measure-

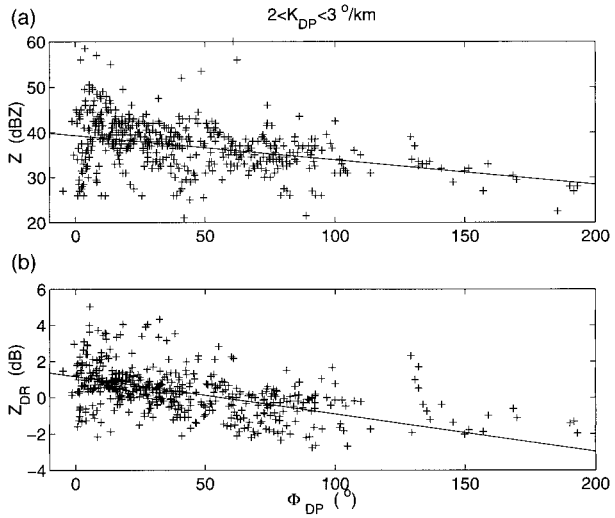


FIG. 4. (a) Scatterplot of $Z_H$ and (b) $Z_{DR}$ against $\Phi_{DP}$ for $2 < K_{DP} < 3$ for C-POL data collected and an elevation of 0.7° at 0449 UTC 28 Nov 1997 during MCTEX. The solid line is a linear regression fit to the data. The slope of the regression is a measure of $A_H$ (a) and $A_{HV}$ (b).

ments, not only is the $Z_H$ measurement affected but differential attenuation is also an important consideration for the measurement of $Z_{DR}$. Since there is an almost linear relation between $\Phi_{DP}$ and the attenuation $A_H$ and $A_{HV}$ (Bringi et al. 1990), changes in reflectivity ($\Delta Z_H$) and differential reflectivity ($\Delta Z_{DR}$) may be approximated by the following (Ryzhkov and Zrnić 1995b):

$$\Delta Z_H = -a\Phi_{DP} \tag{3}$$

and

$$\Delta Z_{DR} = -b\Phi_{DP}. \tag{4}$$

The estimates of $\Phi_{DP}$ have been recalculated by integrating the $K_{DP}$ estimates to remove the effect of backscatter phase jumps for these calculations. Evidence for these relations is shown in Fig. 4 over a narrow range of $K_{DP}$ (2°–3° per km), which corresponds to $47 < Z_H < 50$ dBZ. This narrow range of reflectivity ensures that variations observed are primarily from attenuation effects, assuming a reasonably uniform rain medium so that DSD effects can be neglected on average. The slope of the regression lines in Fig. 4 enables a determination of the constants $a$ and $b$ in Eqs. (3) and (4). This analysis was performed over the entire field of data to have a sufficiently large sample, but some scatter is introduced by variations in beam blockage as a function of azimuth and range. A clear downward trend is evident in both plots (Fig. 4) and for these data $a = 0.08$ dB per degree and $b = 0.02$ dB per degree.

This procedure is robust as long as there exists a reasonable range of $\Phi_{DP}$ to minimize the uncertainty in the fitting procedure. In practice, when this is not the case the attenuation effects are small since attenuation is only significant at large $\Phi_{DP}$. Here $K_{DP}$ values ranging

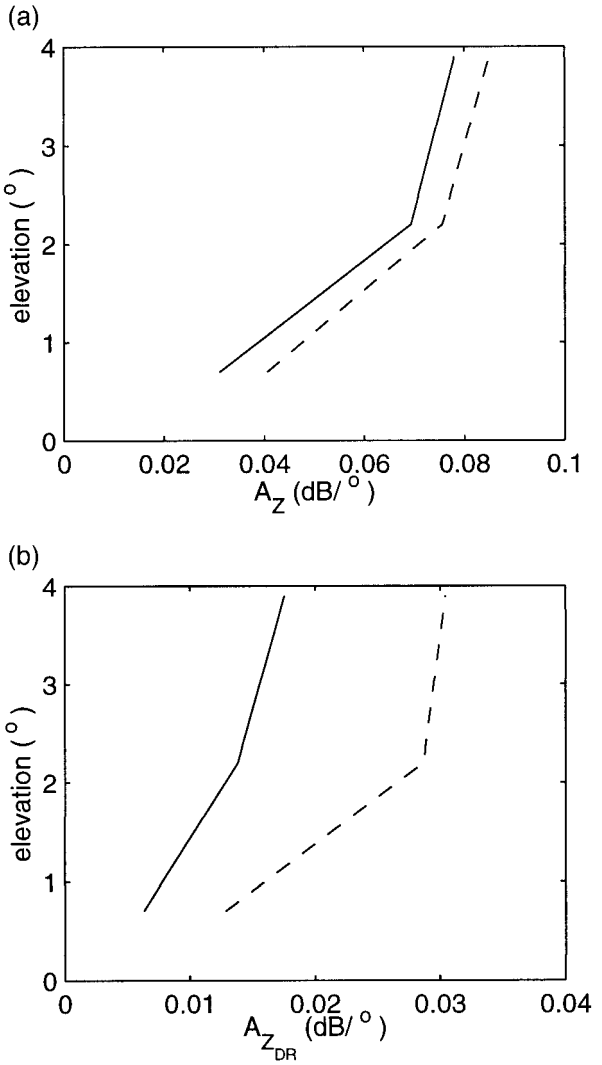


FIG. 5. Profiles of the mean (a) $A_H$ and (b) $A_{HV}$ estimates as a function of elevation tilt angle for the 17 Nov (solid) and 28 Nov (dashed) volume scans.

from 1° to 2° km$^{-1}$ and 2° to 3° km$^{-1}$ were tested. These $K_{DP}$ ranges produce a significant spread of reflectivities (44–50 dBZ) due to DSD variations alone. However, the results in Fig. 4 are not affected to a significant degree by DSD variability alone since the observed variation in $Z_H$ is much larger than the scatter above and there is a clear trend. Furthermore, the results were similar even if the range of values of $K_{DP}$ is set at 0.1° per kilometer intervals starting at 1° km$^{-1}$. Analogous results and conclusions apply to the $Z_{DR}$ data in Fig. 4.

The estimated attenuation coefficients vary significantly from scan to scan and tilt to tilt, as discussed by Carey et al. (1997). The mean attenuation coefficient profiles versus elevation angle for 17 and 28 November 1995 are shown in Fig. 5. The average standard deviation of the $A_Z$ ($A_{Z_{DR}}$) coefficients is 0.015 (0.007) dB per degree. Although there is considerable scatter in the

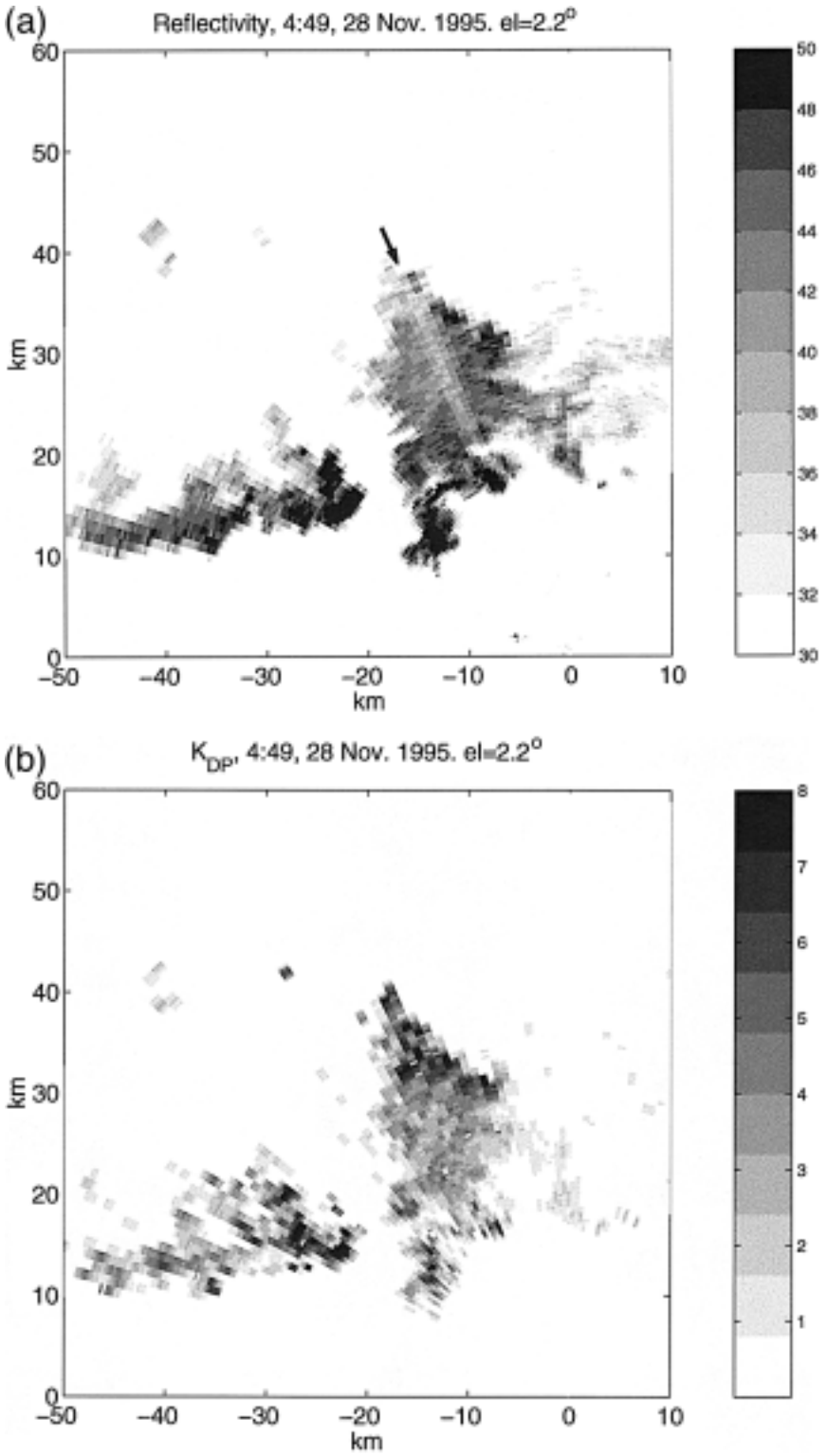


FIG. 6. (a) The $Z_H$ and (b) $K_{DP}$ fields at 0449 UTC 28 Nov 1995 for an elevation of 2.2°. The arrow in (a) denotes ''shadow'' reflectivity zone associated with attenuation through an intense convective core.

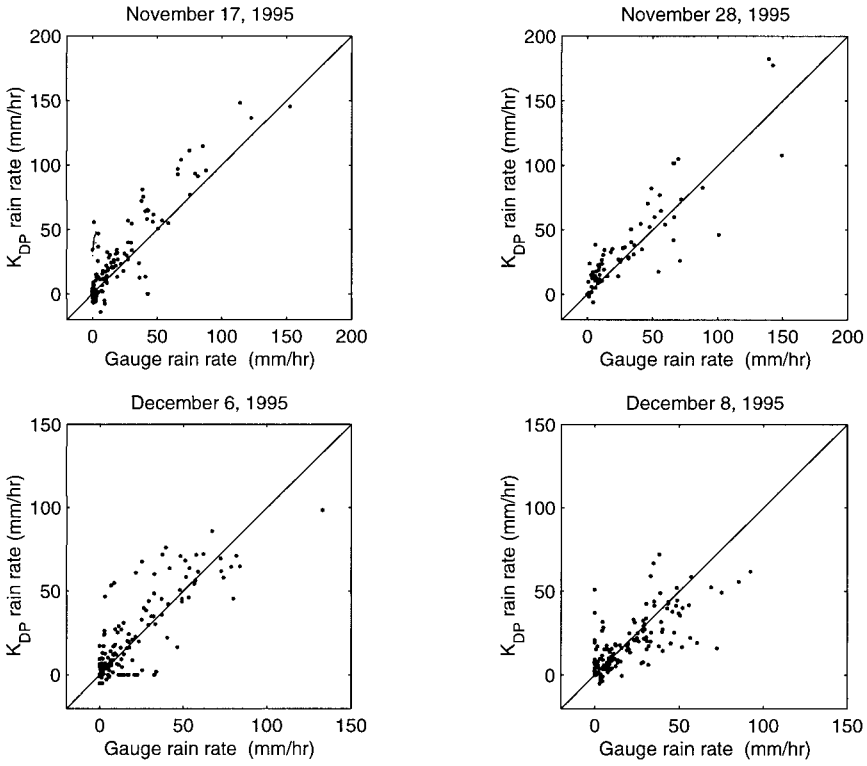


FIG. 7. Comparison of $R(K_{DP})$ and gauge rain-rate estimates for all days using the second tilt angle (1.5°–2.2°).

individual points, the mean profiles are consistent and show that attenuation increases at the larger tilt angles. The attenuation coefficients and their height (and therefore temperature) variations are consistent with the modeling results of Aydin and Giridar (1992) and Keenan et al. (1997).

## 5. Methodology of rain-rate comparison

For this study the radar-derived rain rates were made by first constructing an average of the $K_{DP}$ and $Z_H$ over five consecutive range gates (300 m apart) and five consecutive azimuth rays (a total of 25 values) centered over each rain gauge. The resulting average is a radial average of 2.3 km for the $K_{DP}$ estimates and 1.5 km for the reflectivity-based estimates. At the range of the gauges the azimuth average represents a spatial scale of about 2.2 km. As each $K_{DP}$ estimate is an average over 1.8 km, the five sets of radial $K_{DP}$ information are not independent. The areally averaged radar rainfall estimate is almost matched with the gauge network (one gauge per 5 km$^2$).

TABLE 2. Correlation of radar rain rates with gauge-derived rain rates and slope of least squares regression lines.

| Tilt angle | Cross correlations | | | Slope of best fit | | |
|---|---|---|---|---|---|---|
| | 1 | 2 | 3 | 1 | 2 | 3 |
| Technique | | | | | | |
| $R$–$K_{DP}$ | 0.86 | 0.88 | 0.85 | 1.01 | 1.01 | 0.97 |
| $Z_H$–$R$ | | | | | | |
| NC | 0.72 | 0.67 | 0.62 | 0.17 | 0.41 | 0.45 |
| BC | 0.72 | 0.67 | 0.71 | 0.26 | 0.59 | 0.57 |
| AC | 0.76 | 0.73 | 0.71 | 0.22 | 0.72 | 0.75 |
| All | 0.77 | 0.72 | 0.70 | 0.35 | 0.90 | 0.95 |

NC = no blockage or attenuation correction, BC = blockage correction, AC = attenuation correction, All = blockage and attenuation correction: 1 = 0.7°, 2 = 1.5–2.2°, and 3 = 2.7–3.9°.

The $K_{DP}$ and $Z_H$ values were converted to $R$ using the following relations (Keenan et al. 1997):

$$R(K_{DP}) = 34.6K_{DP}^{0.83}, \quad (5)$$

$$Z_H = 412R(Z)^{1.22}. \quad (6)$$

Equation (5) is based on a raindrop axial ratio relation derived by examination of natural and laboratory rainfall measurements available in the literature. This relation implies that ''natural'' raindrops are slightly less oblate than those obtained with the more traditionally used Pruppacher and Beard (1970) relation. For this reason the constant (34.6) in Eq. (5) is considerably higher than the constant (~20) presented in Aydin and Giridhan (1992). Equation (5) and a $R(K_{DP})$ based on the Prupacher and Beard (1970) oblateness relations have an almost constant ratio, and we will show that the rain-rate data using Eq. (5) agrees very well with

TABLE 3. Mean, standard deviation, and rms differences between rain rates (mm $h^{-1}$) measured by gauges and radar estimates. Data from all four days are included. The radar estimators include $K_{DP}$- and $Z$–$R$-based estimates. Statistics are given for the $Z$–$R$ estimates with and without corrections for beam blockage and attenuation. Time delays of 2, 3, and 4 min are introduced into the gauge data for increasing tilt angles.

| Elevation estimator | 0.7° | | | 1.5–2.2° | | | 2.7–3.9° | | |
|---|---|---|---|---|---|---|---|---|---|
| | Mean | Std dev | rms | Mean | Std dev | rms | Mean | Std dev | rms |
| $R$–$K_{DP}$ | 3.5 | 17.9 | 18.2 | 3.8 | 16.6 | 17.0 | 4.0 | 19.0 | 19.4 |
| $Z_H$–$R$ | | | | | | | | | |
| None | | | | | | | | | |
| Attenuation | −17.7 | 25.8 | 31.2 | −10.1 | 22.7 | 24.9 | −8.2 | 24.6 | 25.9 |
| Blockage | −16.5 | 24.3 | 29.4 | −6.5 | 21.3 | 22.3 | −2.4 | 24.5 | 24.7 |
| Att/block | −14.7 | 23.5 | 27.8 | −4.8 | 23.6 | 24.1 | −4.3 | 26.7 | 27.0 |
| Corrections | −12.9 | 21.5 | 25.1 | 0.3 | 26.3 | 26.3 | 3.1 | 30.2 | 30.4 |

gauge measurements, lending support for the assertion by Keenan et al. (1997) that the Pruppacher and Beard (1970) relation overestimates the oblateness of natural raindrops. Equations (5) and (6) were derived from the disdrometer data collected at the center of the MCTEX rain gauge network shown in Fig. 1.

As discussed previously, C-band attenuation of $Z_H$ and $Z_{DR}$ is a significant problem at 5-cm wavelengths. Often $\Phi_{DP}$ values greater than 100° were observed over the gauges, and values greater than 200° occurred at larger ranges. This corresponds to an attenuation of about 5–10 dB$Z$ in $Z_H$, which obviously would result in a significant bias in $R(Z)$ estimates. Therefore, $Z_H$ data employed for rainfall estimation will be evaluated both with and without the attenuation correction. The attenuation correction employed is based on the observed $\Phi_{DP}$ values, as discussed in the previous section. Note that this technique of attenuation correction is only possible with a polarimetric radar.

Beam blockage significantly affected the lowest tilt angles, as discussed in section 2. For this reason $Z_H$ values used in (6) will be evaluated both with and without blockage corrections.

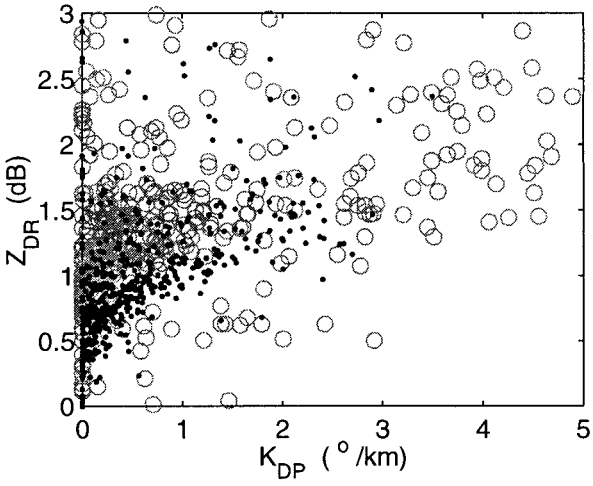


FIG. 8. Scatterplot of $Z_{DR}$ as a function of $K_{DP}$ measured over the gauges for the island (17 Nov 28) cases (○) and oceanic (6 and 8 Dec) cases (·).

For the intercomparison, first the $R(K_{DP})$ estimator (5) will be evaluated. Then $R(Z)$ will be deduced using (6), without any corrections to $Z_H$ [$R(Z)$], with attenuation correction only [$R(Z, A)$], with blockage correction only [$R(Z, B)$], and finally with both blockage and attenuation corrections applied to $Z_H$ [$R(Z, A, B)$].

Obviously there are important sampling issues inherent in the radar–gauge comparisons. The gauge data represent a time average at a particular location. For this study, the $R$ comparisons are based on $R$ derived from gauge data averaged over 5 min. These averages have been calculated centered within 1 min of the radar scan time and with delays of 2, 3, and 4 min to produce a correction for the time taken for the precipitation to reach the ground from the three radar elevations. These delays are incorporated in all the statistics and plots except where explicitly stated otherwise. With the typical advection speeds of storms (5–10 m $s^{-1}$) the 5-min gauge average corresponds to a similar spatial scale inherent in the radar ''box'' averages. The radar estimates of rainfall accumulation are based on the assumption that the radar-derived $R$ was constant over the period between the radar scans. The gauge accumulation at the time of the radar scan was recorded for comparison. The midpoint of the time interval between scans was employed to represent the time of radar rainfall accumulation.

## 6. Radar–gauge comparisons

### *a. Events*

As mentioned, four high rainfall events occurring over the validating gauge network were selected for study. The first two events (17 and 28 November) are good examples of island thunderstorms initially forming on the eastern end of Melville Island and continental in character. Outflows from these initial storms interacted with storms forming on sea-breeze fronts to form westward-moving north–south-aligned multicellular complexes, which moved over the gauge network. An ex-

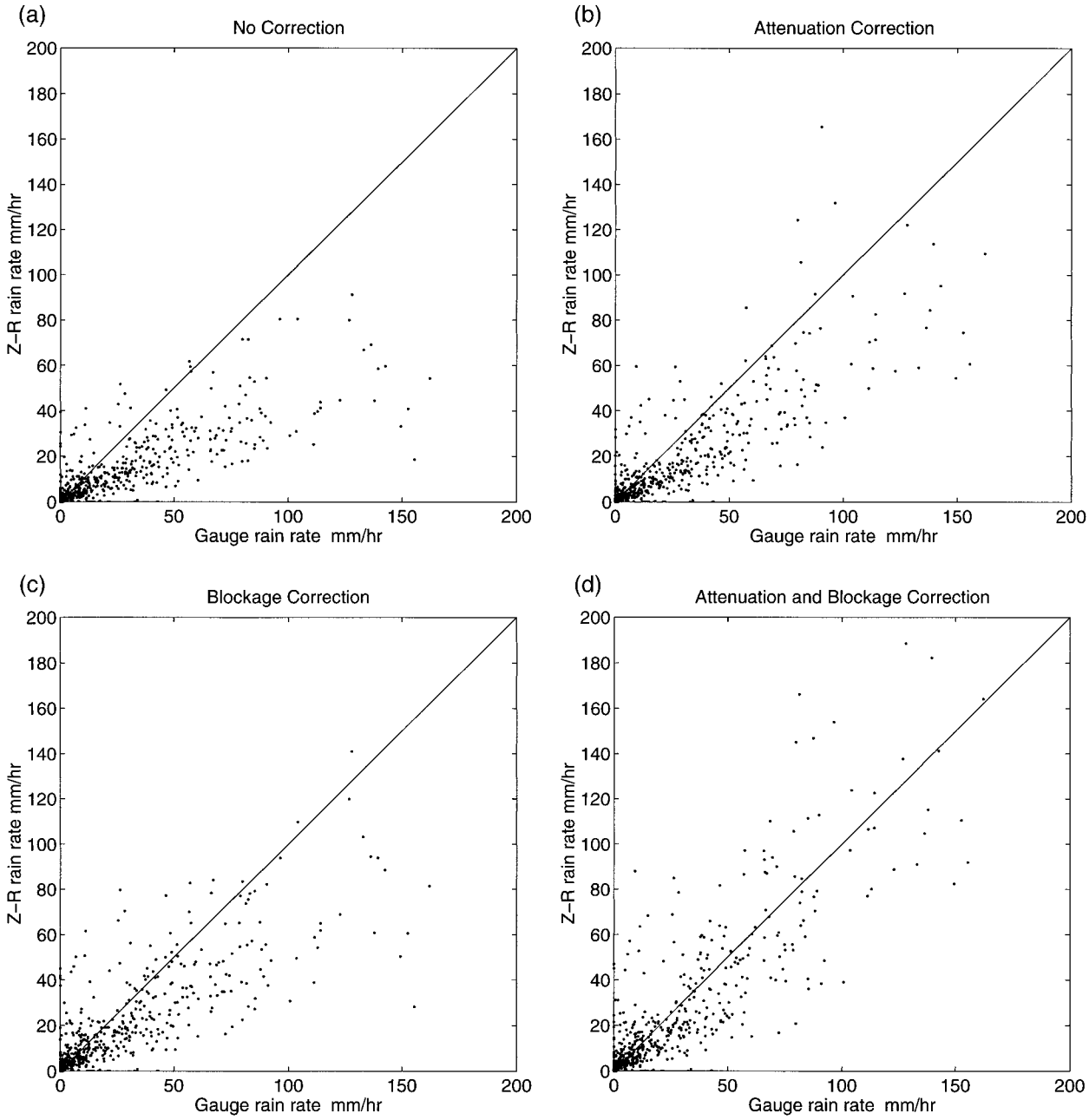


FIG. 9. Comparison of gauge rain rates with collocated radar $Z_H$-based rain-rate estimates for all days from second tilt angle (1.5°–2.2°): (a) no corrections to $Z_H$, (b) employing polarimetric attenuation correction to $Z_H$, (c) employing blocking correction to $Z_H$, and (d) employing both blocking and attenuation corrections to $Z_H$.

ample of the reflectivity and $K_{DP}$ field from the 28 November case is shown in Fig. 6. Strong $K_{DP}$ values are evident in regions of high reflectivity, but the effect of attenuation is also readily apparent. A shadow region of reduced reflectivity is evident behind an intense cell near the radar. However, the largest $K_{DP}$ values are evident within this reflectivity shadow.

The second two events (6 and 8 December) were more consistent with deep oceanic or monsoonal convection. On 6 December, the initial storm development occurred on the northwestern coast of Bathurst Island late in the afternoon. This storm subsequently developed into a multicellular system that moved slowly toward the southeast over the gauge network. On 8 December, a northeast- to southwest-oriented squall line formed offshore in the late afternoon and moved to the southeast. Although a major component of the squall line was offshore, significant rainfall developed over the gauge

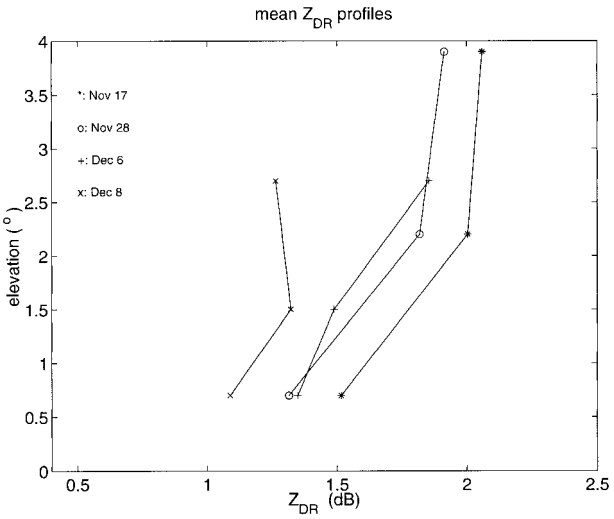


FIG. 10. Vertical profile of mean $Z_{DR}$ over the gauge network.

network. Overall reflectivities were lower for the December cases and this is reflected in the gauge-observed rain rates given in Table 1. The mean (median) rain rate for the periods under consideration is 21.4 (8.7) mm $h^{-1}$.

### *b. Performance of $K_{DP}$-based rain-rate estimators*

A comparison of the individual storm $R(K_{DP})$ estimates from Eq. (5) with the gauge estimates derived for the second tilt angle is shown in Fig. 7. In general, the agreement between the measurements is very good. The scatter is almost independent of rain rate, suggesting that accurate measurements at very high rain rates ($>$150 mm $h^{-1}$) can be made. High values of correlation between the gauge and $R(K_{DP})$ estimates over all four cases are seen (Table 2). There is also little bias evident in $R(K_{DP})$ estimates as a function of elevation angle, shown in Table 3, and a regression line fitted to these $R(K_{DP})$–$R$ data for the whole dataset reveals a slope of almost unity. There is excellent overall agreement over a wide range of $R$ for the four rainfall events with the mean rain-rate error of 3–4 mm $h^{-1}$, as indicated in Table 3. The spread of values for a given rain rate is almost constant as the rain rate increases. Three of the four cases show little or no bias (mean error $<$ 4 mm $h^{-1}$), although the data for 17 November 1995 indicate that the $R(K_{DP})$ values are about 8 mm $h^{-1}$ too high. On average, rms differences between the $R(K_{DP})$ and gauge $R$ values are 13–20 mm $h^{-1}$ for the last 3 days and about 25–30 mm $h^{-1}$ for 17 November. The overall rms differences are less than 20 mm $h^{-1}$. The level of agreement is similar to that expected from Eq. (2) with some allowance for the averaging of the $R(K_{DP})$ estimates. Note that although 25 $K_{DP}$ estimates were used, the estimates along a radial are not independent, so that the effective number of independent samples is just over 5.

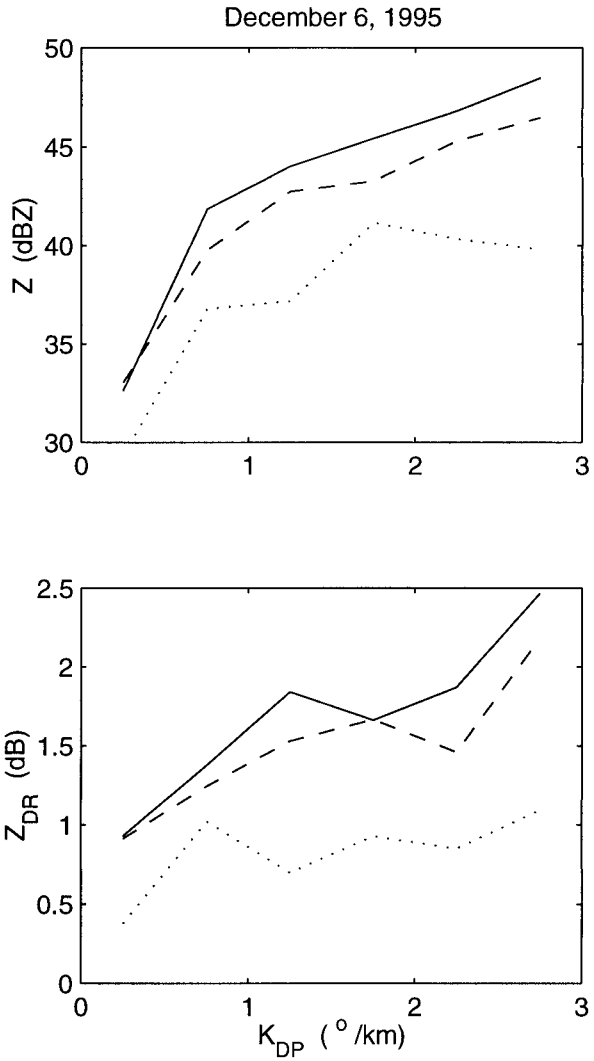


FIG. 11. Plot of $Z_H$ ($Z_{DR}$) vs $K_{DP}$ for the 6 Dec 1995 case. The reflectivities have been corrected for attenuation and beam blockage. The data were grouped in $K_{DP}$ intervals of 0.5° $km^{-1}$ and the median $Z_H$ ($Z_{DR}$) calculated. The radar elevation tilt angles correspond to 0.7° (dotted), 1.5° (dashed), and 2.7° (solid).

The 8–10 mm $h^{-1}$ bias on the 17 November case contributed significantly to larger errors on that day and the overall average rms. The effect is also evident in the accumulation data presented later. Note that the accuracy of the $K_{DP}$ approach for each event is good, even when the rain rate is in excess of 50 mm $h^{-1}$, although there are some differences between the monsoon and island cases, particularly 17 November and 8 December. Figure 8 shows a scatterplot of the $Z_{DR}$ estimates (corrected for differential attenuation) against the $K_{DP}$ over the gauges for the island storms and the oceanic storms. There is a clear offset in the $Z_{DR}$ values for the same $K_{DP}$ by about 0.5 dB. Using the results of Keenan et al. (1997), this corresponds to a change in median volume diameter of the DSDs of about 0.5 mm.

In the above analysis, the $R(K_{DP})$ estimate sometimes

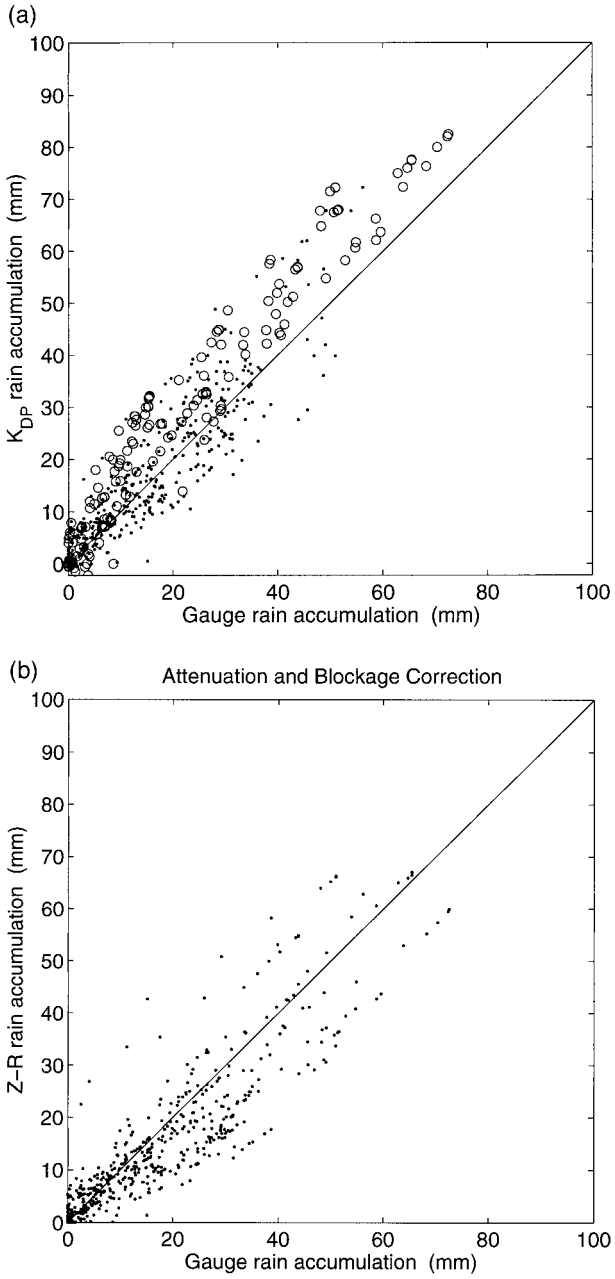


FIG. 12. Comparison of gauge rainfall accumulations with radar-derived estimates derived from second tilt angle (1.5°–2.2°). (a) The $K_{DP}$-based rainfall rates are shown with the 17 Nov data marked as (○) and the remaining data as ( · ). (b) The $Z_H$–$R$ estimates with blockage and attenuation corrections are shown.

produced small negative numbers similar to those reported by Ryzhkov and Zrnić (1996). However, averaged over the period of the storm these low and physically unrealistic negative rain rates are too small to significantly affect the results. Hence with some additional spatial averaging and the use of slightly longer averaging intervals [which produce a $N^{3/2}$ improvement, Eq. (2)], it appears that $K_{DP}$ estimates of $R$ may be useful in the moderate rain rates ($R$ approximately 10 mm h$^{-1}$) often found in stratiform regions. Further work is required to analyze the performance of the $K_{DP}$ estimator at low rain rates.

### c. $Z_H$–$R$ and $K_{DP}$–$R$ rain-rate intercomparisons

Rain rates derived from $Z_H$ consistently underestimate the gauge-derived rain rates (especially at the lower two tilt angles) if corrections to overcome beam blockage and attenuation are not employed. The results shown in Fig. 9 (second tilt angle) and Table 3 illustrate these trends. The use of uncorrected $Z_H$ values biased the $R(Z)$ low at all rain rates and at all tilt angles, although the bias is less with increasing elevation. Use of the attenuation correction results in some improvement, and the blockage correction by itself is even more effective in overcoming the biases. The attenuation correction is more important in the November (island) cases in which the radar was typically sampling rain through more intense convection. In some of these cases $\Phi_{DP}$ values in excess of 200° corresponding to an attenuation of about 16 dB were observed. However, both corrections are necessary to bring the $Z_H$ estimates close to the gauge and $K_{DP}$-based rain-rate values. The best overall $R(Z, A, B)$ are obtained using the second tilt angle (1.4°–1.9°), which results in minimum biases and minima in the standard deviation and rms errors.

The failure of the corrections at the lowest tilt angle is probably related to overwhelming blockage not accounted for in the simple correction procedure. However, there is some evidence that the observed vertical gradient of reflectivity is at least partially microphysical in origin and extends through all three tilts. The vertical gradient of $Z_{DR}$ over the gauges is significant (Fig. 10), suggesting drop breakup is occurring, but no correction for differential blockage is possible. This almost certainly has some effect, as the apparent breakup occurs over a wide area. However, independent disdrometer data are also consistent with some breakup occurring. Inspection of the $Z_H$–$K_{DP}$ and $Z_{DR}$–$K_{DP}$ plots in Fig. 11 also supports the notion of varying microphysical properties of the rain medium at the three tilt angles. For each tilt angle there is evidence for the $Z_H$–$K_{DP}$ and $Z_{DR}$–$K_{DP}$ pairs lying along separate exponential curves; for example, for the higher tilt angles, the $K_{DP}$ values are consistently lower for a given $Z_H$ or $Z_{DR}$. This implies less oblate drops or a larger number of smaller drops. This is consistent with the hypothesis that breakup of drops is under way.

The cross-correlation maxima for all the cases are less than those obtained with the $K_{DP}$ rain-rate estimates. The improvement in the $R(Z)$ correlations are mostly associated with corrections for attenuation—an effect primarily seen in data from the island storms. Of interest is a tendency for the best correlation to occur at time lags slightly larger (1–2 min) than the best agreement for the $R(K_{DP})$ estimates. This is not related to the dif-

TABLE 4. Rainfall accumulation errors.

| Elevation estimator | 0.7° | | | 1.5–2.2° | | | 2.7–3.9° | | |
|---|---|---|---|---|---|---|---|---|---|
| | Mean | Std dev | rms | Mean | Std dev | rms | Mean | Std dev | rms |
| $K_{DP}$ | 2.1 | 6.8 | 7.1 | 1.6 | 7.0 | 7.2 | 2.0 | 8.3 | 8.6 |
| $Z_H$–$R$ | | | | | | | | | |
| None | | | | | | | | | |
| Att. correction | −12.2 | 12.8 | 17.7 | −7.8 | 9.3 | 12.1 | −6.6 | 9.0 | 11.2 |
| Blockage–corr. | −11.5 | 12.1 | 16.7 | −5.8 | 7.5 | 9.5 | −3.4 | 7.8 | 8.5 |
| Att/block | −10.5 | 11.4 | 15.5 | −4.8 | 7.8 | 9.2 | −4.4 | 8.3 | 9.4 |
| Correction | −9.5 | 10.3 | 14.0 | −2.2 | 7.0 | 7.4 | −0.4 | 8.4 | 8.4 |

ferent dependencies on drop diameter of $Z_H$ and $K_{DP}$. If this was the case, the $R(Z)$ correlations should maximize at smaller lags as the reflectivity is more sensitive to larger drops (and hence higher fall speeds) compared with $K_{DP}$. Rather, it appears to be associated with the error growth modified by the exponent in the $Z$–$R$ relation. If an extreme value of the exponent, such as 2–2.5, is used, the correlation maximizes at a similar lag to the $R(K_{DP})$. The maximum correlation is also higher and the rms errors reduced for such a power dependence, but low rain rates are severely biased (N.B. a bias in rain rate does not affect the correlation values, and we are dealing mostly with high rain rates in this dataset).

Even with all corrections applied, the $R(Z, A, B)$ estimates have substantially more spread than observed with $R(K_{DP})$ estimates (cf. the spread in Figs. 7 and 9 and the standard deviation and rms errors in Table 3). The time variation of $R$ was captured well by the $R(K_{DP})$ approach and reasonably well with the $R(Z)$ approaches at least with blockage and attenuation corrections applied as indicated in Table 2. These correlations support the concept that the main problem with the $Z_H$-based $R$ estimates was one of getting the correct magnitude of $R$. This level of agreement may also be expressed as fractional and mean standard errors where the rms and mean differences in Table 3 are normalized with respect to the mean rain rate. For the second tilt these are 70% (110%) and 8% (1%), respectively, for the $R(K_{DP})$ [$R(Z, A, B)$].

As the previous analysis indicates, there does not appear to be one simple answer to the question of what is affecting the traditional $Z_H$-based rainfall rate estimates. In this case corrections made for beam blockage and attenuation effects substantially improved the overall accuracy. However, some of the differences probably result in part from microphysical evolution within the measured precipitation. In other words a height-dependent $Z_H$–$R$ relation allowing for the vertical evolution of the DSD is possibly warranted. For the lowest tilt angle of 0.7°, a quite extreme relation of $Z_H = 120R^{1.4}$ is necessary to eliminate the observed biases.

Hence with appropriate corrections, including the polarimetric-based attenuation corrections and allowing for time lags, traditional $Z_H$-based rainfall estimates are able to provide reasonable rainfall estimates.

### *d. Rainfall accumulation intercomparisons*

The intercomparison of the radar-based rainfall accumulations with the gauge accumulations at the time of each scan for all four days is shown in Fig. 12, and results for each tilt angle are summarized in Table 4. The plots support the results presented previously. From Table 4 the mean difference in the $K_{DP}$ accumulation estimates is always positive, indicating a slight tendency for the $K_{DP}$ approach to overestimate the accumulated rainfall. Most of this bias is associated with the 17 November case (○ in Fig. 12). Accumulation errors based on $K_{DP}$ range from about 12%–15% on average and do not vary significantly with the tilt used. For the $R(Z, A, B)$ estimates the tendency is for optimal agreement at the second tilt angle with the attenuation and blockage correction applied. There remains a bias, which is slightly larger than the $K_{DP}$ accumulation bias. However, these overall statistics need to be qualified because the case with the worst $K_{DP}$ performance has the most data points, while the case with the worst $Z$ statistics (28 November) had the least (and poorer time resolution). When the areal-averaged accumulations are plotted (Fig. 13), it is clear that on some occasions the $R(Z, A, B)$ is severely biased, particularly the data from 28 November. This is also the smallest sample and it is probable that if comparable time resolution data were available, the overall $Z$-based accumulations would show greater bias. The mean error is only 6.5% of the total, but, as indicated in Fig. 13, there is considerably more variability in the areal-averaged total rainfall accumulation by the end of each event in the $Z_H$-based approaches than in the polarimetric $K_{DP}$ approach. The average of the absolute difference between the radar and gauge estimates at the end of each event and the corresponding fractional standard error (defined as the rms difference–mean accumulation) are given in Table 5. These again attest to the excellent agreement between the gauge and $K_{DP}$ accumulation estimates.

On a daily basis, a much larger accumulation bias was evident with the $K_{DP}$ estimates on 17 November. The mean difference ($R - G$) was about 6 mm compared with −1, −2, and 0.1 mm on 28 November, 6 December, and 8 December, respectively. The $Z_H$–$R$ estimate with

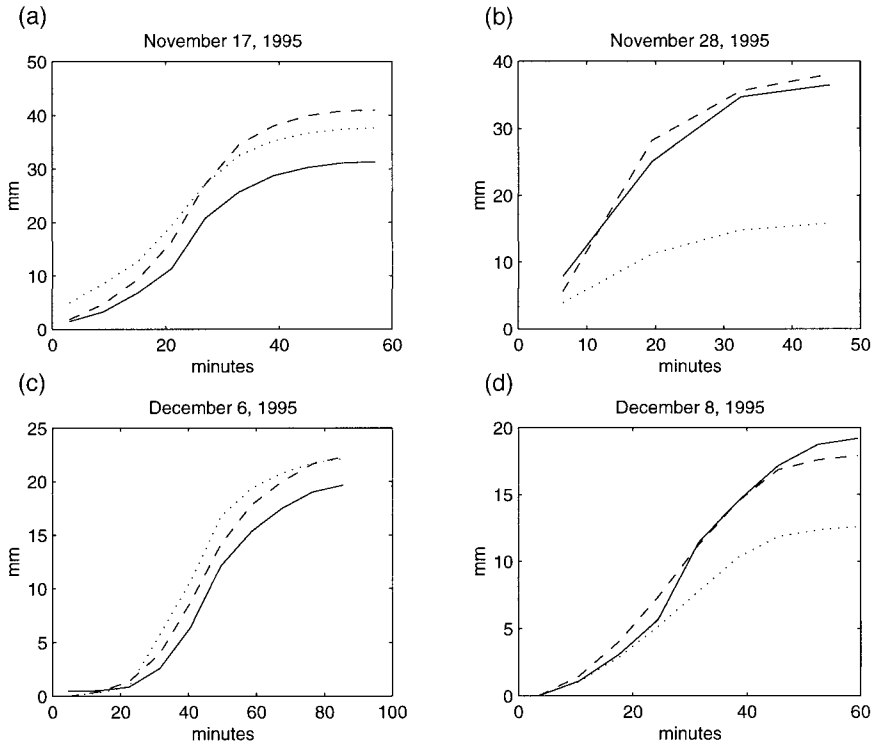


FIG. 13. Average rainfall accumulation over the gauge network vs time as measured by gauges (heavy line), $R(K_{DP})$ (dashed), and $R(Z, A, B)$ (dotted) at an elevation of ~2° for (a) 17 Nov, (b) 28 Nov, (c) 6 Dec, and (d) 8 Dec.

attenuation and blockage correction also had corresponding mean differences of 1, −6, −3, and −3 mm.

## 7. Conclusions

This paper has examined the use of a polarimetric C-band (5-cm wavelength) radar for rainfall measurements with the primary focus on $K_{DP}$- and $Z$-based estimators. The use of polarimetric measurements have considerable potential advantages compared with conventional radar observations. In particular, the phase-based estimators are immune to beam blockage and attenuation effects (Ryzhkov and Zrnić 1996) and simulations suggest that the polarimetric variables are less sensitive to drop size distribution (DSD) effects (Keenan et al. 1997). C-band systems offer some advantages over polarimetric S-band radars as they have smaller antennas for a given angular resolution and the differential propagation phase is approximately twice that observed at S band. However, there are significantly more questions resulting from important resonance-scattering effects (Keenan et al. 1997). A new consensus-based $K_{DP}$ estimator has been used in these analyses since the sensitivity to resonance scatter effects occasionally produce significant backscatter phase discontinuities.

TABLE 5. Mean absolute difference and relative error of the accumulation averaged over the gauge network at the end of each of the four heavy rain events.

| | Mean absolute difference 1.5°–2.2° | Fractional standard error |
|---|---|---|
| $R(K_{DP})$ | 3.8 mm | 21% |
| $R(Z, A, B)$ | 9.0 mm | 49% |

The $R(K_{DP})$ estimates have been compared with data from 20 rain gauges, and overall excellent agreement has been shown. The overall statistics show relatively small rms differences and essentially unbiased rain estimates with very high cross correlation between the gauge and $R(K_{DP})$ data. This includes periods with very high rain rates, exceeding 150 mm $h^{-1}$. However, some sensitivity to DSD effects remain evident. For example, data from 17 November had a bias toward higher rain rates. The mean $Z_{DR}$'s observed over the gauges were systematically larger on this day, indicating larger median drop diameters. This indicates that a dual $K_{DP}$–$Z_{DR}$ estimator (Jameson 1991a; Ryzhkov and Zrnić 1995a) may offer some advantages in similar rain regimes.

The $R(Z)$ and $R(Z, B)$ estimates were all heavily biased. However, when a polarimetric-based attenuation correction was applied, good agreement was obtained at the upper two elevations (2.2° and 3.9° for two cases; 1.5° and 2.7° for the other two cases). Beam blockage effects in the lowest tilt had overwhelming consequences, although there may also have been some microphysical influence on the chronic underestimation of

rain rate. The rms differences between radar and gauges for the $R(Z, A, B)$ are larger than those for the $R(K_{DP})$ estimates by about 50%; a result that is also reflected in lower cross correlations. Variations from case to case associated with variations in mean DSD characteristics were more pronounced in the $Z$-based estimates.

Overall, the polarimetric rainfall estimation at C band is extremely promising, particularly for medium to high rain rates. Nevertheless, further analysis of more cases is needed to fully document the sensitivity to drop size distributions.

*Acknowledgments.* The support of the Tiwi Land Council in undertaking MCTEX is acknowledged. We also thank NCAR for the loan of the antenna and pedestal used in C-POL. NCAR is sponsored by the National Science Foundation. This work was also supported by NASA through Contracts NAG5-2692 and NAG5-4754 to Colorado State University.

## REFERENCES

Aydin, K. H., and V. Giridhar, 1992: C-band dual polarization radar observables in rain. *J. Atmos. Oceanic Technol.,* **9,** 383–390.

——, H. Direskeneli, and T. Seliga, 1987: Dual-polarization radar estimation of rainfall parameters compared with ground-based disdrometer measurements: October 29, 1982 central Illinois experiment. *IEEE Trans. Geosci. Remote Sens.,* **6,** 834–844.

——, Y. Lure, and T. A. Seliga, 1990: Polarimetric radar measurements of rainfall compared with ground-based rain gauges during MAYPLOE'84. *IEEE Trans. Geosci. Remote Sens.,* **28,** 443–449.

Balakrishnan, N., and D. S. Zrnić, 1990: Estimation of rain and hail rates in mixed-phase precipitation. *J. Atmos. Sci.,* **47,** 565–583.

Battan, L. J., 1973: *Radar Observations of the Atmosphere.* University of Chicago Press, 324 pp.

Blackman, M., and A. J. Illingworth, 1995: Improved measurement of rainfall using differential phase techniques. *Proc. Int. Seminar COST 75 Weather Radar Systems,* Brussels, Belgium, Commission of the European Communities, 662–771.

Bringi, V. N., S. M Cherry, M. P. M. Hall, and T. A. Seliga, 1978: A new accuracy in determining rainfall rates and attenuation due to rain by means of dual-polarization measurements. *IEEE Conf. Publ.,* **169** (2), 120–124.

——, T. A. Seliga, and S. M. Cherry, 1982: First comparison of rainfall rates derived from radar differential reflectivity and disdrometer measurements. *IEEE Trans. Geosci. Remote Sens.,* **2,** 201–204.

——, V. Chandrasekar, N. Balakrishnan, and D. S. Zrnić, 1990: An examination of propagation effects in rainfall on radar measurements at microwave frequencies. *J. Atmos. Oceanic Technol.,* **7,** 829–840.

Carey, L. D., S. A. Rutledge, and T. D. Keenan, 1997: Correction of attenuation and differential attenuation at S- and C-Band using differential propagation phase. Preprints, *28th Conf. on Radar Meteorology,* Austin, TX, Amer. Meteor. Soc., 25–26.

Chandrasekar, V., V. N. Bringi, N. Balakrishnan, and D. S. Zrnić, 1990: Error structure of multiparameter radar and surface measurements of rainfall. Part III: Specific differential phase. *J. Atmos. Oceanic. Technol.,* **7,** 621–629.

——, V., E. Gorgucci, and G. Scarchilli, 1993: Optimization of multiparameter radar estimates of rainfall. *J. Appl. Meteor.,* **32,** 1288–1293.

Fischer, M. A., and R. C. Bolles, 1981: Random sample consensus: A paradigm for model fitting with applications to image analysis and automated cartography. *Commun. Assoc. Comput. Mach.,* **24,** 381–395.

Goddard, J. W. F., and S. M Cherry, 1984: The ability of dual-polarization radar (coplanar linear) to predict rainfall rate and microwave attenuation. *Radio Sci.,* **19,** 201–208.

Golestani, Y., V. Chandrasekar, and V. N. Bringi, 1989: Intercomparison of multiparameter radar measurements. Preprints, *24th Conf. on Radar Meteorology,* Tallahassee, FL, Amer. Meteor. Soc., 309–314.

Gorgucci, E., G. Scarchilli, and V. Chandrasekar, 1996: Operational monitoring of rainfall over the Arno River Basin using dual-polarization radar and rain gauges. *J. Appl. Meteor.,* **35,** 1221–1230.

Hildebrand, P. H., 1978: Iterative correction for attenuation of 5 cm radar in rain. *J. Appl. Meteor.,* **17,** 508–514.

Holt, A. R., 1988: Extraction of differential propagation phase from S-band circularly polarized radars. *Electron. Lett.,* **24,** 1241–1242.

Hubbert, J. V., and V. N. Bringi, 1995: An iterative filtering technique for the analysis of coplanar differential phase and dual-frequency radar measurements. *J. Atmos. Oceanic Technol.,* **12,** 643–648.

——, V. Chandrasekar, and V. N. Bringi, 1993a: Processing and interpretation of coherent dual-polarized radar measurements. *J. Atmos. Oceanic Technol.,* **10,** 155–164.

——, J. Caylor, and V. Chandrasekar, 1993b: A practical algorithm for the estimation of Doppler velocity and differential phase from dual polarization radar measurements. *Proc. 26th Int. Conf. on Radar Meteorology,* Norman, OK, Amer. Meteor. Soc., 112–114.

Jameson, A. R., 1991a: A comparison of microwave techniques for measuring rainfall. *J. Appl. Meteor.,* **30,** 32–54.

——, 1991b: Polarization radar measurements in rain at 5 and 9 GHz. *J. Appl. Meteor.,* **30,** 1500–1513.

Keenan, T. D., and Coauthors, 1994: Science plan-maritime continent thunderstorm experiment. BMRC Research Rep. 44, 61 pp. [Available from BMRC, GPO Box 1289K, Melbourne, Vic. 3001, Australia.]

——, D. Zrnić, L. Carey, P. May, and S. Rutledge, 1997: Sensitivity of C-band polarimetric variables to propagation and backscatter effects in rain. Preprints, *28th Conf. on Radar Meteorology,* Austin, TX, Amer. Meteor. Soc., 13–14.

——, K. Glasson, F. Cummings, T. S. Bird, J. Keeler, and J. Lutz, 1998: The BMRC/NCAR C-Band polarimetric (C-POL) radar system. *J. Atmos. Oceanic Technol.,* **15,** 871–886.

Marshall, J. S., and W. M. Palmer, 1948: The distribution of raindrops with size. *J. Meteor.,* **5,** 165–166.

Meischner, P. F., V. N. Bringi, D. Heimann, and H. Holler, 1991: A squall line in southern Germany: Kinematics and precipitation formation as deduced by advanced polarimetric and Doppler radar measurements. *Mon. Wea. Rev,* **119,** 678–701.

Mueller, E. A., 1984: Calculation procedures for differential propagation phase shift. Preprints, *22d Conf. on Radar Meteorology,* Zurich, Switzerland, Amer. Meteor. Soc., 397–399.

Pruppacher, H. R., and K. V. Beard, 1970: A wind tunnel investigation of the internal circulation and shape of water drops falling at terminal velocity in air. *Quart. J. Roy. Meteor. Soc.,* **96,** 247–256.

Ryzhkov, A., and D. S. Zrnić 1995a: Comparison of dual-polarization radar estimators of rain. *J. Atmos. Oceanic Technol.,* **12,** 249–256.

——, and ——, 1995b: Precipitation and attenuation measurement at a 10-cm wavelength. *J. Appl. Meteor.,* **34,** 2121–2134.

——, and ——, 1996: Assessment of rainfall measurement that uses specific differential phase. *J. Appl. Meteor.,* **35,** 2080–2090.

Sachidananda, M., and D. S. Zrnić, 1986: Differential propagation phase shift and rainfall estimation. *Radio Sci.,* **20,** 907–922.

——, and ——, 1987: Rain rate estimates from differential polarization measurements. *J. Atmos. Oceanic Technol.,* **4,** 588–598.

Scarchilli, G., E. Gorgucci, V. Chandrasekar, and T. A. Seliga, 1993: Rainfall estimation using polarimetric techniques at C-Band frequencies. *J. Appl. Meteor.,* **32,** 1150–1160.

Seliga, T. A., and V. N. Bringi, 1976: Potential use of a radar differential reflectivity measurements at orthogonal polarizations for measuring precipitation. *J. Appl. Meteor.*, **15,** 69–76.

——, and ——, 1978: Differential reflectivity and differential phase shift: Applications in radar meteorology. *Radio Sci.*, **13,** 271–275.

——, ——, and H. H. Al-Khatib, 1981: A preliminary study of comparative measurements of rainfall rate using the differential reflectivity technique and a raingauge network. *J. Appl. Meteor.*, **20,** 1362–1368.

Ulbrich, C. W., and D. Atlas, 1984: Assessment of the contribution of differential polarization to improved rainfall measurements. *Radio Sci.*, **19,** 49–57.

Zahrai, A., and D. S. Zrnić, 1993: The 10 cm-wavelength polarimetric weather radar at NOAA's National Severe Storms Laboratory. *J. Atmos. Oceanic Technol.*, **10,** 649–662.

Zawadzki, I., 1986: Factors affecting the precision of radar measurements of rain. *Proc. 22d Conf. on Radar Meteorology*, Snowmass, CO, Amer. Meteor. Soc., 251–256.

Zrnić, D. S., and A. Ryzhkov, 1996: Advantages of rain measurements using specific differential phase. *J. Atmos. Oceanic Technol.*, **13,** 454–464.